Transactions on Environment, Energy and Earth Sciences
ISSN: 2960-1924, eISSN: 2960-2300 | Volume 5
EMCEME 2025

Mechanistic Insights into Heterocyclic Diels–Alder Reactivity and Selectivity

Yixuan Feng

Department of Chemistry, Universiti Malaya, Kuala Lumpur, Malaysia

23053893@siswa.um.edu.my

Abstract. Heterocyclic dienes such as furan, pyrrole, and thiophene expand the synthetic versatility of the Diels–Alder (DA) reaction but often deviate from classical Frontier Molecular Orbital (FMO) predictions. Small endo–exo gaps, dearomatization penalties, and retro-DA pathways render outcomes highly sensitive to subtle physical factors beyond orbital symmetry. This review synthesizes recent advances by employing the activation strain model (ASM) and energy decomposition analysis (EDA), complemented by natural orbital for chemical valence (NOCV) channel analysis and transition-state asynchronicity (Δr_TS). Comparative studies benchmark carbocyclic versus heterocyclic systems, quantify substituent and positional effects, and map catalytic modes—including Lewis acids, hydrogen-bond donors, and ion-pair catalysts—onto Δ(ΔE_Pauli/ΔV_elstat/ΔE_orb). Case studies, particularly the furan–maleic anhydride manifold, reveal that endo control in benchmarks is largely strain-dominated, whereas rate modulation in heterodienes frequently originates from Pauli-repulsion reduction and asynchronous transition states. A harmonized framework addressing solvent, temperature, reference state, free versus electronic energies, intrinsic reaction coordinate validation, and conformer handling is presented, together with a unified comparison table. The resulting guidelines connect mechanistic insights to rational design in synthetic, pharmaceutical, and materials chemistry, while identifying priorities for future research.

Keywords: Diels–Alder reaction; heterocyclic diene; activation strain model; energy decomposition analysis; endo–exo selectivity.

1. Introduction

The Diels–Alder (DA) cycloaddition is a cornerstone of molecular construction owing to its high atom economy, ability to generate multiple stereocenters in a single step, and broad tolerance of substitution patterns [1]. The incorporation of heterocyclic dienes such as furan, pyrrole, and thiophene further broadens its scope, offering compatibility with renewable feedstocks (e.g., furfural derivatives), access to bioactive scaffolds, and tunable reversibility that is useful in polymeric and stimuli-responsive materials [2–4]. However, heterodienes also introduce additional energetic complexities, including dearomatization penalties, attenuated endo–exo selectivity, and non-negligible retro-DA rates, all of which complicate predictive design [3, 5]. In recent years, research has moved beyond qualitative Frontier Molecular Orbital (FMO) and Secondary Orbital Interaction (SOI) arguments toward physically resolved models that disentangle strain and interaction contributions and trace the physical origins of selectivity [6–8]. Despite these advances, several challenges remain. In prototypical systems such as furan with maleic anhydride, FMO/SOI theory predicts a strong endo preference, whereas experimental and high-level computational studies consistently report only small endo–exo gaps, suggesting that secondary-orbital rationales alone fail to capture the full energetic balance [3, 5]. Emerging analyses highlight decisive roles for Pauli repulsion, electrostatics, orbital interactions, fragment strain, and transition-state asynchronicity (Δr_TS), factors that are insufficiently represented in frontier-orbital treatments [6–8]. Moreover, cross-system datasets rarely employ harmonized conditions of solvent, temperature, and standard state, nor do they consistently report key metrics such as ΔG‡(endo/exo) and ΔΔG‡, hindering mechanistic generalization and quantitative benchmarking [5]. Against this backdrop, the objectives of the present review are threefold: first, to identify the physical determinants of reactivity and selectivity in heterocyclic DA reactions beyond classical FMO theory; second, to quantify substituent

and positional effects through activation strain model (ASM), energy decomposition analysis (EDA), and natural orbital for chemical valence (NOCV) methods, with particular emphasis on Δr_TS; and third, to map catalytic strategies—including Lewis acids, hydrogen-bond donors, and ion pairs—onto changes in ΔE_Pauli, ΔV_elstat, and ΔE_orb, thereby distilling design rules and proposing standardized reporting practices. Clarifying these mechanistic drivers is significant because it can directly reduce activation free energies (ΔG‡), restore predictable endo/exo control, and enable deliberate management of retro-DA processes. Such insights are relevant not only to synthetic methodology but also to catalyst development in pharmaceutical and materials chemistry, particularly within sustainable platforms that use biomass-derived heterodienes and green solvents. We hypothesize that electronic and steric tuning can shift the ASM balance between strain and interaction, promoting earlier and more asynchronous transition states that reduce ΔE_strain and Pauli repulsion, thereby lowering barriers and re-establishing selectivity. The remainder of this paper is structured as follows: Section 4 synthesizes classical and recent advances and highlights research gaps; Section 5 outlines inclusion and normalization criteria; Section 6 summarizes the mechanistic toolkit (ASM, EDA, NOCV, Δr_TS); Section 7 presents comparative analyses of benchmark systems, substituent and positional effects, catalytic strategies, and model–experiment audits; and Section 8 concludes with priorities for future directions.

2. Literature Review

2.1. Existing research overview

Classical FMO/SOI reasoning successfully rationalizes many carbocyclic systems, particularly where endo control correlates with favorable secondary orbital interactions and steric arrangements [6–7]. However, heterocycles frequently exhibit small endo–exo differences and lower intrinsic reactivity due to dearomatization and diminished strain discrimination [3, 5]. The activation strain model (ΔE = ΔE_strain + ΔE_int) provides a transparent decomposition of barriers along the intrinsic reaction coordinate and has shown that endo preferences in benchmarks such as cyclopentadiene + maleic anhydride originate primarily from smaller ΔE_strain at the endo TS [6–8]. In the reaction between furan and maleic anhydride, the overall barriers are higher and the endo–exo gap is modest. Energy decomposition analysis reveals weaker orbital stabilization and minimal strain advantage, consistent with limited selectivity and a tendency toward reversibility, as shown in Figure 3 [2–3]. Beyond furan, recent studies on pyrrole and thiophene confirm a similar trend. Variation in heteroatom identity alters donor/acceptor balance and ring aromaticity, thereby shifting the interplay between strain and interaction terms, reducing endo biases, and increasing sensitivity to substituent effects and catalytic conditions [3, 8]. These insights align with the broader move toward physically interpretable, quantitatively benchmarked models for DA selectivity [6–8].

2.2. Research gaps

Standardized datasets. Standardized datasets reporting ΔG‡(endo/exo), ΔΔG‡, Δr_TS, and EDA components under consistent solvent, temperature, and standard-state conditions remain scarce, particularly for pyrrole and thiophene [3]. Reversibility (k_forward, k_reverse or K_eq) is inconsistently reported [2]. Model gaps. FMO-centric narratives underweight Pauli repulsion, electrostatics and asynchronicity; comparative ASM/EDA studies across heterocycles using matched computational protocols remain limited [6–8]. Dispersion effects are occasionally treated as part of the general interaction term rather than being analyzed as distinct contributors. Asymmetric heterodiene DA. Asymmetric heterodiene Diels–Alder reactions with quantitative mechanistic validation remain underexplored, and the development of catalytic fingerprints that correlate Δ(ΔE_Pauli/ΔV_elstat/ΔE_orb) with ΔΔG‡ or enantioselectivity (ee) is still needed [6–8].

2.3. Relevance to this study

In this review, all units are standardized to kcal·mol⁻1, with a clear distinction made between free and electronic energies, and explicit reporting of solvent, temperature, and standard state is recommended. This review integrates ASM/EDA with Δr_TS and experimental findings to derive actionable design rules and propose a concise reporting checklist aimed at improving reproducibility.

3. Literature Screening Method

This review employed a systematic literature screening strategy to ensure consistency and comparability across the studies analyzed. Publications from 2010 to 2025 were surveyed using databases such as Web of Science, Scopus, and Google Scholar. The search employed keywords including "Diels–Alder," "heterocyclic dienes," "furan," "pyrrole," "thiophene," "activation strain," "energy decomposition," "asynchronicity," and "Lewis acid catalysis." Studies were prioritized when they provided mechanistic decompositions using approaches such as the activation strain model (ASM), energy decomposition analysis (EDA), or natural orbital for chemical valence (NOCV), alongside kinetic or thermodynamic data [6–9]. Articles were included when they reported key mechanistic parameters—such as ΔG‡(endo/exo), ΔΔG‡, ΔE_Pauli, ΔV_elstat, ΔE_orb, or Δr_TS—with solvent and temperature conditions explicitly stated; papers lacking such mechanistic or energetic detail were excluded [3]. To facilitate comparability, all reported values were standardized to kcal·mol⁻¹, and particular attention was given to studies conducted under consistent solvent and temperature conditions or those explicitly discussing the sensitivity of results to variations in these parameters. The review also synthesized common computational practices reported across the surveyed literature. Geometries and vibrational frequencies were frequently optimized at density functional theory (DFT) levels such as M06-2X/def2-TZVPP, with single-point refinements at higher levels when available (e.g., DLPNO-CCSD(T)//DFT) [10–13]. Energy decomposition analyses were typically performed at ZORA-DFT/TZ2P or comparable levels, often in combination with NOCV [6–9]. Dispersion corrections (e.g., DFT-D3) were generally included and, where discussed, evaluated separately from primary interaction-energy components [12]. These methodological details reflect trends in the literature and are presented here in a comparative and descriptive manner rather than as original calculations.

4. Mechanistic Models and Concepts

Activation-strain analysis. Activation-strain diagrams are interpreted to diagnose whether reactivity trends are strain-controlled or interaction-controlled [6–8]. Endo biases can originate from smaller ΔE_strain at the endo TS (e.g., sterics that disfavor exo deformation) [6–8]. For heterocycles, reduced strain discrimination and altered orbital interactions diminish endo–exo differences and elevate the role of Pauli repulsion [2–3, 5]. (Figure 1) [3].Energy decomposition and NOCV channels. EDA assigns physical origins to ΔE_int changes—closed-shell Pauli repulsion, classical electrostatics, and stabilizing orbital interactions—while NOCV exposes donor/back-donor pathways (e.g., HOMO(diene)→LUMO(dienophile) versus reverse donation) [6–9]. Rate enhancements under Lewis-acid catalysis often track with a reduction in Pauli repulsion and an increase in electrostatic stabilization [6–8]. (Figure 2) [8].Asynchronicity (Δr_TS). Increased Δr_TS typically lowers ΔE_strain by reaching the TS earlier/asymmetrically [6–8, 13]. Donor substitution and substituent position (2- vs 3-) frequently modulate Δr_TS; strategic catalysts can also increase asynchronicity and reduce ΔG‡ [3, 5, 14].Dispersion. Local energy-decomposition studies indicate dispersion contributions are generally modest and slowly varying along ζ in DA; they should be evaluated but not conflated with the primary drivers of reactivity/selectivity differences [12].

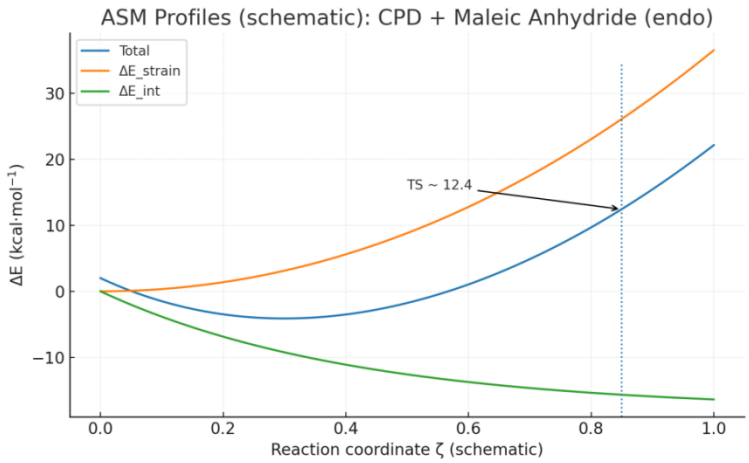

Figure 1: ASM profiles (schematic) for cyclopentadiene + maleic anhydride

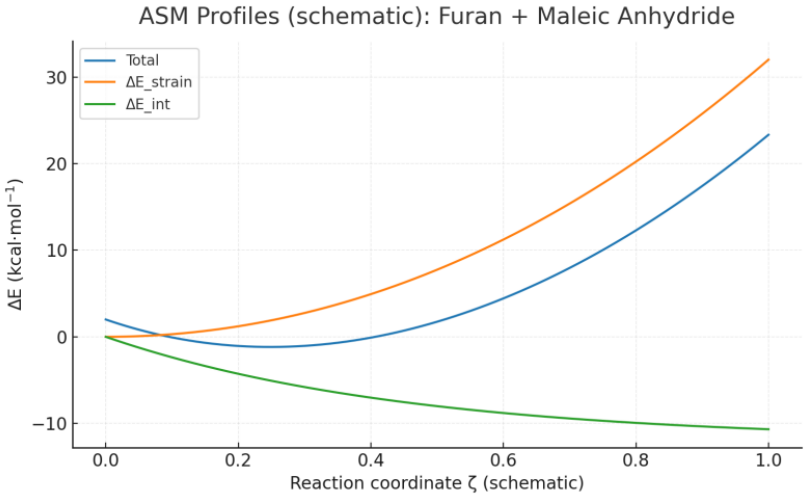

Figure 2: ASM profiles (schematic) for furan + maleic anhydride

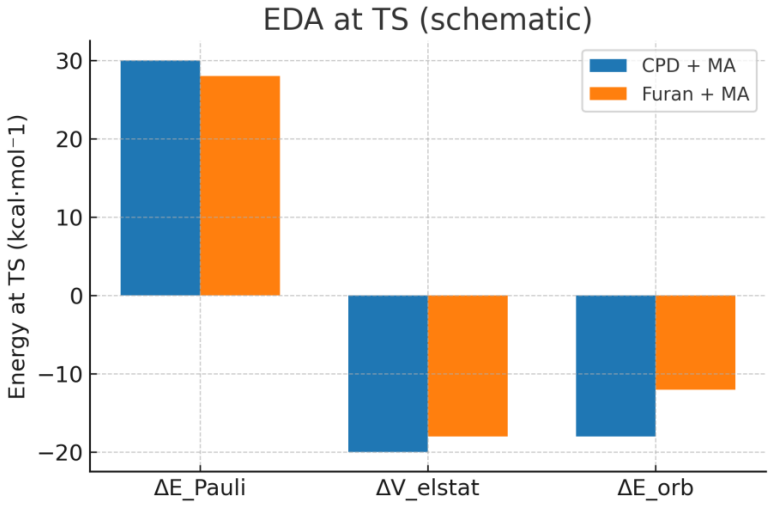

Figure 3: EDA component comparison at TS (schematic) for cyclopentadiene vs furan

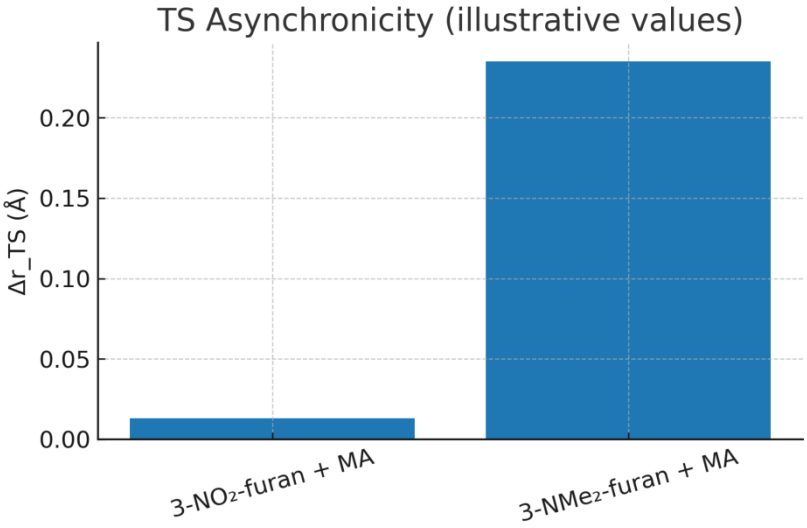

Figure 4: Transition-state asynchronicity Δr_TS for representative substituted furans

Figure 1 (CPD + maleic anhydride): Endo is strain-controlled—endo TS has smaller ΔE_strain; ΔE_int is similar → ΔG‡_endo lower. [6–8]. Figure 2 (Furan + maleic anhydride): Higher barriers and small endo–exo gap from weaker ΔE_orb and reduced strain discrimination; Pauli matters more; reversibility is common. [2–3, 15–17].Figure 3 (Furan endo/exo & reversibility): System is near-iso-selective; retro-DA competes; solvent/temperature/catalysis toggle kinetic vs thermodynamic control. [2–3, 18]. Figure 4 (Substituent × position rules): Donor/acceptor × 2/3-position reshapes ΔE_Pauli and Δr_TS, enabling endo↔exo flips; design via substituent–position–dienophile matrices. [3, 5, 14, 17].

5. Results and Comparative Discussion

5.1. Benchmarks

Carbocyclic dienes versus heterodienes [3, 7–8]. Cyclopentadiene + maleic anhydride remains the archetype for endo control, where ASM shows a clear strain advantage for the endo TS and EDA reveals similar or slightly more favorable interaction for the exo pathway [6–8]. Furan + maleic anhydride, in contrast, exhibits a higher barrier and a small endo–exo gap, consistent with weaker ΔE_orb and reduced strain discrimination; this reaction is frequently reversible under practical conditions [2–3]. The contrast illustrates that endo control in carbocycles is not directly transferable to heterocycles without reassessing the strain/interaction balance [3, 6–8].

5.2. Heterocycle classes

Furan, pyrrole and thiophene. Across these classes, the heteroatom identity governs both the ease of dearomatization and the polarization of the diene π-system [3, 8, 15]. Furans often show modest endo biases and manageable barriers that are strongly substitution-sensitive [3]. Pyrrole tends to exhibit higher barriers due to stronger aromatic stabilization and charge distribution, leading to sluggish kinetics unless assisted by catalysts or strong dienophiles [15]. Thiophene, being more aromatic, often shows the greatest dearomatization penalty and a pronounced need for activation (e.g., Lewis acids) or electronically activated dienophiles [16]. As a trend, moving from furan → pyrrole → thiophene increases reliance on Pauli-repulsion management and Δr_TS engineering to access practical rates [6–8, 14].

5.3. Substituent×position rules (furan exemplar, extension to others)

Substituent identity (donor vs acceptor) and position (2– vs 3–) can invert endo/exo preferences by reshaping the interaction–strain trade-off [3, 5–8, 14]. Strong donors (e.g., NMe_2) commonly lower ΔE_Pauli and increase Δr_TS, thereby reducing ΔG‡ and favoring endo in some positions; strong acceptors (e.g., NO_2) tend to elevate ΔE_Pauli and reduce asynchronicity [3, 5, 14]. Notably, 2- versus 3- substitution can flip the orientation where steric alignment and early/late TS timing diverge [3]. While the detailed magnitudes are system-specific, the design implication is general: chart a matrix of substituent electronics × position × dienophile electronics and use ASM/EDA/Δr_TS to pre-bias the pathway before experimental screening. (Figure 4) [17]. (Figure 5) [5].

5.4. Catalysis fingerprints: Lewis acid

Hydrogen-bond and ion-pair catalysis. Many catalytic manifolds can be classified by their characteristic impact on EDA components [6–8]. Lewis acids often compress ΔE_Pauli (by reorganizing electron density and lowering occupied–occupied clashes), increase ΔV_elstat, and can enhance ΔE_orb; hydrogen-bond donors achieve a milder version of the same pattern; ion pairs combine electrostatics with organizational effects. These fingerprints provide a practical guide to choose catalysts not merely by frontier-gap heuristics but by the expected Δ(components) signature, particularly when selectivity amplification is the goal [2, 19]. (Figure 6) [18].

5.5. Applications: synthesis, green chemistry and materials

Biomass-derived furfural engages in DA with maleimides and other activated dienophiles under bio-based solvents such as 2-MeTHF, highlighting the intersection of mechanism and sustainability [2, 4, 20]. Polymer/materials applications exploit retro-DA to achieve self-healing or thermally reversible linkages; in these contexts, understanding ΔE_strain, ΔE_Pauli and Δr_TS informs the temperature windows where assembly/disassembly can be toggled [6–8, 14, 18–19]. For pharmaceutical settings, catalyst choice guided by EDA/ASM fingerprints can reduce temperature and improve selectivity to minimize protecting-group manipulations [6–8].

5.6. Model–experiment audit and reporting checklist

To reconcile mechanistic claims with experimental observables, we recommend: (i) specify functional/basis/dispersion and confirm TS by IRC [10, 12–13, 21]; (ii) distinguish free vs electronic energies and state temperature and standard state [10, 22]; (iii) define solvent models [23]; (iv) enumerate conformers and apply Boltzmann weighting where relevant [22]; (v) quantify reversibility (k_forward, k_reverse or K_eq) and concentration effects on retro-DA [2]; (vi) define Δr_TS with bond labels and discuss dispersion separately from ΔE_int drivers [12, 14]. These steps materially improve cross-study comparability and error diagnosis

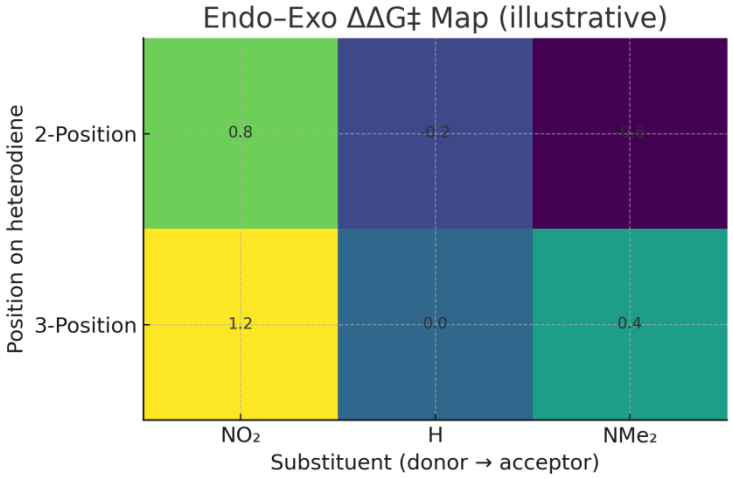

Figure 5: Substituent×position heat map for endo–exo bias (ΔΔG‡, illustrative template)

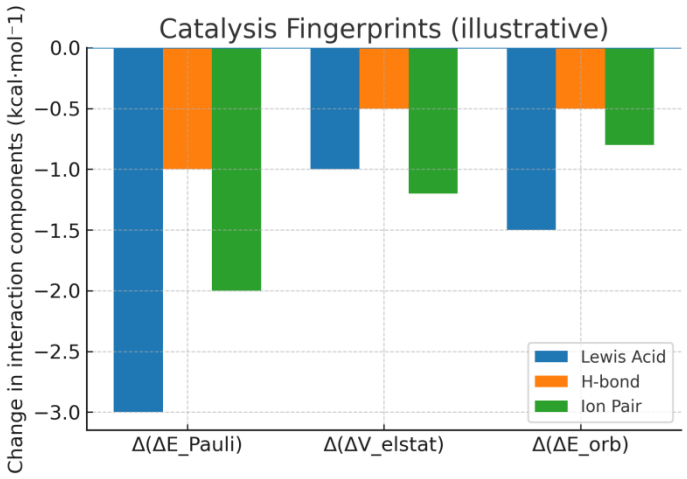

Figure 6: Catalysis fingerprints: Δ(ΔE_Pauli/ΔV_elstat/ΔE_orb) under different catalytic modes

This table compiles benchmark and substituted-furan systems under a unified reporting convention (kcal·mol⁻¹), including ΔG‡_endo/ΔG‡_exo, the selectivity gap ΔΔG‡ = ΔG‡_endo – ΔG‡_exo, solvent/temperature/standard state, and concise ASM/EDA annotations (qualitative trends in ΔE_Pauli/ΔV_elstat/ΔE_orb and Δr_TS). Entries marked "n.r." denote values not reported in a directly comparable form. The goal is rapid, like-for-like comparison of endo/exo control and substituent×position effects across sources [1–3, 6].

Table 1: Unified comparison—benchmarks and substituted furans (representative values; kcal·mol⁻1)

System (dienophile)	Solvent / T	ΔG‡_endo / ΔG‡_exo	ΔΔG‡ (endo–exo)	Key note	Δr_TS (Å)
Cyclopentadiene + maleic anhydride	n.r.	n.r.	+2.2 (endo)	Smaller deformation at endo TS	n.r.
Furan + maleic anhydride	n.r.	n.r.	~+0.4–0.6 (endo)	Weaker bonding; minimal strain advantage; reversible	n.r.
3-NO_2-furan + maleic anhydride	n.r.	n.r.	−1.2 (exo)	Interaction–strain trade-off	0.149
3-NMe_2-furan + maleic anhydride	n.r.	n.r.	+1.7 (endo)	Repulsion lowering; asynchronous TS	0.235
2-NO_2-furan + maleic anhydride	n.r.	n.r.	+1.2 (endo)	Interaction favors endo	n.r.
2-NMe_2-furan + maleic anhydride	n.r.	n.r.	+0.6 (exo)	Lower repulsion along exo path	n.r.

Notes: n.r. = not reported in a unified format across sources; entries summarize tendencies reported across representative literature.

Parent furan + maleic anhydride: barriers are higher and ΔΔG‡ is small, consistent with weaker ΔE_orb and reduced strain discrimination; this aligns with the frequently observed (partial) reversibility [2–3].

Substituent effects (furan): strong donors (e.g., NMe_2) at C-3 often lower ΔE_Pauli and increase Δr_TS, thereby lowering ΔG‡ and sometimes enhancing endo; strong acceptors (e.g., NO_2) tend to raise ΔE_Pauli and dampen asynchronicity, potentially raising barriers or weakening endo, depending on position/conjugation [3, 5, 14].2- vs 3-position: when steric alignment and early/late TS timing diverge, endo/exo orientation can flip; interpreting Δr_TS together with ΔE_Pauli is essential [3].

Methodological consistency: differences in solvent, temperature, standard state, and electronic-structure level (e.g., M06-2X/def2-TZVPP; DLPNO-CCSD(T)//DFT) can introduce systematic shifts; this table normalizes units/conditions where possible to improve comparability [10–11, 13].

In summary: for furan manifolds, the tunable levers are ΔE_Pauli and Δr_TS; substituent×position is the key dial for rate and endo control [3, 6–8].

This qualitative matrix summarizes furan / pyrrole / thiophene trends: intrinsic reactivity and endo–exo tendencies, dearomatization penalties, and the dominant ASM/EDA levers (e.g., Pauli-repulsion management and Δr_TS engineering). It also flags when systems are more catalyst-dependent (Lewis acids, H-bond donors, ion pairs) or prefer electronically activated dienophiles. The aim is a compact design guide for choosing conditions across heterocycles and dienophile electronics [1–5].

Table 2: Comparative tendencies—pyrrole and thiophene (qualitative trends; kcal·mol^{-1} where available)

Heterodiene	General ΔG‡ trend	Endo–exo tendency	Dearomatization burden	Key ASM/EDA lever	Notes
Furan	Lower vs pyrrole/thiophene	Small endo bias	Moderate	ΔE_orb weaker; ΔE_strain similar	Often reversible; substitution-sensitive
Pyrrole	Higher than furan	Very small endo bias	Higher	Pauli and electrostatics dominate	Catalyst/strong dienophiles helpful
Thiophene	Highest of the three	Minimal intrinsic bias	Highest	Pauli-repulsion management essential	Activation or strong LA often required

Across heterocycles: moving furan → pyrrole → thiophene increases aromatic stabilization and dearomatization cost, raising ΔG‡ and attenuating intrinsic endo bias. Control shifts from strain discrimination toward Pauli-repulsion management and Δr_TS engineering; reliance on catalysis correspondingly grows [3, 6–8, 18].Selectivity & reversibility: furan typically shows modest ΔΔG‡ and can be reversible/partially reversible; pyrrole/thiophene more often require strong dienophiles or catalysis to achieve practical rates/selectivities [2–3, 15].Design implication: start on furan to map substituent×position×dienophile rules that transfer; for pyrrole/thiophene, apply catalysis fingerprints (e.g., ↓ΔE_Pauli, ↑ΔV_elstat, ±ΔE_orb) and target Δr_TS to pre-bias outcomes [6–8, 18, 20–23].In summary: heterocycles are not a simple extrapolation of carbocycle rules; endo/exo control must be re-balanced using ASM/EDA levers and Δr_TS-guided optimization [3, 6–8].

6. Conclusion

The outcomes of heterocyclic Diels–Alder reactions arise from a delicate balance between fragment deformation and interaction components. In carbocyclic systems such as cyclopentadiene, endo selectivity is typically dominated by strain effects, whereas in heterodienes the reduced strain

discrimination and weaker orbital stabilization attenuate endo preferences and shift control toward Pauli repulsion and transition-state asynchronicity (Δr_TS). The combined use of activation strain model (ASM), energy decomposition analysis (EDA), and natural orbital for chemical valence (NOCV) transforms qualitative Frontier Molecular Orbital (FMO) concepts into quantitative design principles, clarifying why donor/acceptor substitution and positional effects can invert endo/exo selectivity. Dispersion forces, although non-negligible, generally contribute in a modest and slowly varying manner and should be considered independently of primary drivers. Looking forward, several priorities emerge. In the short term (0–2 years), the establishment of harmonized datasets for furan, pyrrole, and thiophene—including ΔG‡, ΔΔG‡, Δr_TS, and EDA components under explicitly defined solvent, temperature, and reference-state conditions—together with curated substituent–position–dienophile matrices and standardized reporting checklists, will be essential for cross-study comparability. In the medium term (2–5 years), systematic development of "catalysis fingerprints" that correlate changes in Pauli repulsion, electrostatics, and orbital interactions with ΔΔG‡ and enantioselectivity (ee) for Lewis-acid, hydrogen-bond, and ion-pair platforms will help rationalize and expand catalytic strategies. In the longer term (>5 years), the creation of computationally efficient predictors trained on ASM, EDA, Δr_TS, and aromaticity descriptors, and their prospective validation in pharmaceutical, materials, and green-chemistry applications, offers a path toward mechanistically informed and sustainable design of heterocyclic Diels–Alder reactions.

7. References

[1] Mackay, E. G.; Claridge, T. D. W.; Anderson, E. A. The Diels–Alder Reaction in Steroid Synthesis. Synthesis 2015.

[2] Cioc, R. C.; et al. The Interplay between Kinetics and Thermodynamics in the Reversible Furan Diels–Alder Reaction. ChemSusChem 2022.

[3] Alves, T. V.; Fernández, I. Understanding the Reactivity and Selectivity of Diels–Alder Reactions Involving Furans. Org. Biomol. Chem. 2023, 21, 7767–7775.

[4] Galkin, K. I.; Ananikov, V. P. Intermolecular Diels–Alder Cycloadditions of Furfural-Based Chemicals from Renewable Resources. Int. J. Mol. Sci. 2021, 22, 11856.

[5] Ho, G. M.; et al. Unconventional exo Selectivity in Thermal Normal-Electron-Demand Diels–Alder Reactions. Sci. Rep. 2016.

[6] Bickelhaupt, F. M.; Houk, K. N. Analyzing Reaction Rates with the Distortion/Interaction–Activation Strain Model. Angew. Chem. Int. Ed. 2017.

[7] Fernández, I.; Bickelhaupt, F. M. The Activation Strain Model and Molecular Orbital Theory: Understanding and Designing Chemical Reactions. Chem. Soc. Rev. 2014.

[8] Vermeeren, P.; Hamlin, T. A.; Bickelhaupt, F. M. Chemical Reactivity from an Activation Strain Perspective. Chem. Commun. 2021, 57, 5880–5896.

[9] Mitoraj, M. P.; Michalak, A.; Ziegler, T. A Combined Charge and Energy Decomposition Scheme for Bond Analysis (ETS-NOCV). J. Chem. Theory Comput. 2009, 5, 962–975.

[10] Zhao, Y.; Truhlar, D. G. The M06 Suite of Density Functionals… (including M06-2X). Theor. Chem. Acc. 2008, 120, 215–241.

[11] Riplinger, C.; Neese, F. Natural Triple Excitations in Local Coupled Cluster Calculations with Pair Natural Orbitals (DLPNO-CCSD(T)). J. Chem. Phys. 2013, 139, 134101.

[12] Grimme, S.; Antony, J.; Ehrlich, S.; Krieg, H. A Consistent and Accurate ab initio Parametrization of DFT-D (DFT-D3). J. Chem. Phys. 2010, 132, 154104.

[13] Weigend, F.; Ahlrichs, R. Balanced Basis Sets (def2-SVP/TZVP/TZVPP/QZVPP) for H to Rn. Phys. Chem. Chem. Phys. 2005, 7, 3297–3305.

[14] Vermeeren, P.; Hamlin, T. A.; Bickelhaupt, F. M. Origin of Asynchronicity in Diels–Alder Reactions. Proc. Natl. Acad. Sci. U.S.A. 2021, 118, e2105314118.

[15] Yadav, V. A Computational Study of the Relative Aromaticity of Pyrrole, Furan, Thiophene and Selenophene, and Their Diels–Alder Stereoselectivity. ChemRxiv 2020, preprint, 10.26434/chemrxiv.12734039.v1.

[16] Calvo-Martín, G.; Plano, D.; Sanmartín, C. New Experimental Conditions for Diels–Alder and Friedel–Crafts Alkylation Reactions with Thiophene… Molecules 2022, 27, 982.

[17] Lee, M. W.; Stille, J. K. Stereochemistry of the Furan–Maleic Anhydride Cycloaddition. J. Org. Chem. 1978, 43, 518–524.

[18] Fortunato, G.; Etienne, D.; Bogdan, P.; et al. Advances in Self-Healing Coatings Based on Diels–Alder Chemistry. Polymer 2024, 287, 126281.

[19] Ratwani, C. R.; et al. Self-Healing by Diels–Alder Cycloaddition in Advanced Polymeric Materials. Prog. Polym. Sci. 2023.

[20] Skolia, E.; et al. Direct Diels–Alder Reaction of Biomass-Derived Furfurol with Maleimides in a Bio-Based Solvent, 2-MeTHF. Eur. J. Org. Chem. 2024, e202400105.

[21] Gonzalez, C.; Schlegel, H. B. An Improved Algorithm for Reaction Path Following. J. Chem. Phys. 1990, 94, 5523–5527. (IRC)

[22] Luchini, G.; Alegre-Requena, J. V.; Funes-Ardoiz, I.; Paton, R. S. GoodVibes: Automated Thermochemistry for Computational Chemistry. F1000Research 2020, 9, 291.

[23] Marenich, A. V.; Cramer, C. J.; Truhlar, D. G. Universal Solvation Model (SMD). J. Phys. Chem. B 2009, 113, 6378–6396.